



Haemodynamic analysis of vessel remodelling in STA-MCA bypass for Moyamoya disease and its impact on bypass patency



Feng-Ping Zhu^{a,b,1}, Yu Zhang^{a,1}, Masakazu Higurashi^a, Bin Xu^b,
Yu-Xiang Gu^b, Ying Mao^{b,*}, Michael Kerin Morgan^a, Yi Qian^{a,*}

^a Australian School of Advanced Medicine, Macquarie University, Sydney, Australia

^b Department of Neurosurgery, Hua Shan Hospital, Fudan University, Shanghai, China

ARTICLE INFO

Article history:

Accepted 21 March 2014

Keywords:

Moyamoya disease
STA-MCA bypass
Flow resistance
Computational fluid dynamic

ABSTRACT

The purpose of this study is to estimate the remodelling characteristics of STA-MCA bypass and its influence on patency via the use of computational fluid dynamic (CFD) technology. The reconstructed three-dimensional geometries from MRA were segmented to create computational domains for CFD simulations. Eleven patients, who underwent regular MRA both immediately following surgery and at the six months follow-up, were studied. The flow velocities at STA were measured via the use of quantitative MRA (QMRA) to validate simulation results. STA-MCA bypass patency was confirmed for each patient immediately following surgery. The simulation indicated that the remodelling of the arterial pedicle in nine patients was associated with a reduction in the resistance to flow through the bypass. For these cases, the modelling of a driving pressure of 10 mmHg through the bypass at 6 months post-surgery resulted in a 50% greater blood flow than those found immediately following surgery. However, two patients were found to exhibit contradictory patterns of remodelling, in which a highly curved bending at the bypass immediately post-surgery underwent progression, with increased resistance to flow through the bypass at 6 months follow-up, thereby resulting in a modelled flow rate reduction of 50% and 25%, respectively. This study revealed that STA-MCA bypass has a characteristic remodelling that usually reduces flow resistance. The initial morphology of the bypass may have had a significant effect on the outcome of vessel remodelling.

© 2014 Elsevier Ltd. All rights reserved.

1. Introduction

Moyamoya disease is a cerebrovascular disorder characterized by progressive occlusion of arteries around the internal carotid artery bifurcation, which was first reported by Takeuchi and Shimizu (1957). This occlusion results in the formation of collaterals from a fine vascular network at the base of the brain called Moyamoya vessels, responsible for the “puff of smoke” appearance on angiography, from which the name is derived (Fukui, 1997; Suzuki and Takaku, 1969). Despite extensive collateralisation, the clinical manifestation of infarction and haemorrhage may ensue. In order to ameliorate these complications, bypass surgery is often indicated (Kuroda and Houkin, 2008). Though there is still some argument about whether bypass surgery is useful for the treatment of occluded cerebrovascular disease due to atherosclerosis, direct STA-MCA bypass combined with or without indirect revascularization is often performed for Moyamoya patients to reduce the risk of cerebral

ischemic or haemorrhagic stroke by flow augmentation and collateralisation reduction (Kuroda and Houkin, 2008; Zhao et al., 2007). However, spontaneous changes to the bypass from the time that the STA-MCA bypass is established are expected in the first few weeks and even months following surgery. Such auto-remodelling may modify the final outcome of the treatment.

The objective of this paper is to estimate vessel auto-remodelling following STA-MCA bypass surgery via the use of CFD. We carried out CFD analysis on eleven patients with Moyamoya disease treated by STA-MCA anastomosis, with subsequent follow-up by Magnetic Resonance Angiography (MRA) to capture auto-remodelling and observed flow resistance modifications due to its effect on the bypass flow rate. The change in the wall shear stress (WSS) occurring at the bypass due to auto-remodelling was also calculated.

2. Methods

2.1. Patient information

Eleven consecutive adult patients with ages ranging from 24 to 47 years were examined by MRA after undergoing STA-MCA bypass surgery and at 6 months following surgery. All patients were diagnosed with Moyamoya disease and treated

* Corresponding author. Tel.: +61 2 98123551; fax: +61 298123610.

** Corresponding author. Tel./fax: +862152888771.

E-mail addresses: maoying@fudan.edu.cn (Y. Mao), yi.qian@mq.edu.au (Y. Qian).

¹ Authors Feng-Ping Zhu and Yu Zhang contributed equally to this article.

with combined STA-MCA bypass and encephaloduromyosynangiosis (EDMS) at Huashan Hospital from 2010 to 2012 (Xu et al., 2012). Anterior and/or posterior branch of STA were anastomosed to the cortical branch of MCA in an end-to-side fashion. The demographic features of patient details are listed in Table 1. All protocol was approved of by the Institutional Research and Ethics Committee of Huashan hospital. Each participant provided written informed consent.

Three-dimensional (3D) geometries of bypasses were reconstructed and segmented via use of commercial software package - MIMICS (Materialise' Interactive Medical Image Control System) to create domain for CFD computation.

QMRA, which was implemented with Non-invasive Optimal Vessel Analysis (NOVA) software (VasSol Inc., Chicago, Illinois, USA), was performed to measure the blood flow of the STA (Amin-Hanjani et al., 2007, 2013). In this study, the inflow rate of the STA immediately following surgery was measured to be at an average of 37.7 ml/min.

2.2. Surgical procedures

A modified pterional approach was adopted. The branches of the STA could be observed on the medial surface of the flap, with the dissociated anterior and/or posterior branches of the STA (donor artery) pulled through the temporal muscle to the vicinity of the target arteries for anastomosis. The STA was washed with pressurized normal saline containing heparin to relieve spasms, and then anastomosed with the cortical branch of MCA in an end-to-side fashion using a single 10-0 nylon atraumatic suture. Additional EDMS and dural pedicle insertion was performed as described in previous papers (Xu et al., 2012).

2.3. CFD modelling

Three-dimensional (3-D) geometry bypass was built via generation of two-dimensional contours from grey scales of pixels, and by subsequent interpolation in a normal direction. This method prevents the intrusion of surface noise. Rather than utilising "global smoothing", we used manual "local smoothing" to keep 3-D geometries as realistic as possible. This method exhibited an average error of approximately one-third of a pixel in size (Jamali et al., 2007).

Conservation equations for 3-D steady flow with rigid walls were solved via use of the CFX finite-volume-based CFD solver in the ANSYS 14.0 package (Ansys Inc., Canonsburg, PA, USA), with flow considered under steady state conditions. It has been established that steady state simulation may provide similar time-averaged results for pulsatile calculations over a cardiac cycle (Kim et al., 2008).

Grid independence validations have been carried out in our previous work (Qian et al., 2010; Zhang et al., 2012a). The total grid number was selected from a value between 600,000 and 800,000 for each case. In order to accurately measure WSS at the near-wall-region, the body-fitted prism layers were generated close to the vessel walls to improve the resolution of the relevant scales in fluid motion. The distance from the first layer to the vessel surface was fixed at 0.01 mm, whilst prism layer thickness was set to 0.2 mm. From the centre of the vessels to the prism inner layer, the size of the grid was seen to gradually decrease. In order to simulate peripheral capacitance, the outlet of the vessel was extended distally in the normal downstream direction to 100 mesh layers, sufficient for the recovery of blood pressure. A zero pressure condition was used at the outlets. In order to form a fully developed flow boundary layer at the proximal inlet, the domains were extended in an upstream direction to 20 times the size of STA, so that fully developed velocity profiles were able to form in the boundary layer.

Table 1 Clinical characteristics of the patients and the bypass diameter and flow results.

Case	Sex, age	Clinical onset	Surgical side	Immediate post surgery		Follow up		Flow resistance (immediate post surgery)		Flow resistance (follow up)	
				Bypass diameter	Bypass flow	Bypass diameter	Bypass flow	A	B	A	B
A	F, 30	Ischemic stroke	Rt	0.44	22	1.35	33	0.0082	0.270	0.0013	0.190
B	M, 44	TIA	Lt	1.08	30	1.97	100	0.0025	0.260	0.0006	0.045
C	M, 46	Ischemic stroke	Rt	1.23	43	2.19	75	0.001	0.140	0.001	0.064
D	M, 45	Ischemic stroke	Lt	1.66	40	1.50	55	0.0037	0.120	0.0015	0.110
E	F, 24	Ischemic stroke	Lt	2.10	42	1.60	100	0.002	0.044	0.0007	0.020
F	M, 34	TIA	Lt	1.54	39	1.92	85	0.0008	0.107	0.0008	0.060
G	M, 38	Hemorrhagic stroke	Rt	1.77	44	1.73	65	0.0017	0.117	0.001	0.085
H	M, 35	Hemorrhagic stroke	Lt	1.00	15	1.69	35	0.010	0.484	0.005	0.097
I	F, 43	Ischemic stroke	Lt	1.14	35	1.00	80	0.002	0.092	0.0012	0.089
J	M, 45	TIA	Lt	1.78	35	1.60	15	0.0023	0.153	0.0044	0.593
K	F, 47	Ischemic stroke	Rt	1.11	70	1.09	45	0.0003	0.049	0.0002	0.104

F: Female; M: Male; TIA: Transient ischemic attack; Rt: Right; Lt: Left, Bypass diameter (mm), Bypass flow (ml/min).

2.4. Bypass flow resistance

It is known that under the same pressure drop, the conduit with lower flow resistance will have a higher blood flow rate; i.e. better patency. The bypass conduit from STA to MCA is irregular in geometry, with vessel auto-remodelling modifying the morphology of the bypass and thereby flow resistance as well. By measuring bypass flow resistance, the effect of auto-remodelling to the bypass patency may potentially be estimated. Based on pipe flow theory (Brater and King, 1976), pressure drop within a vessel can be expressed as having the following relationship with flow

$$\Delta p = Am^2 + Bm \tag{1}$$

where *m* is the mass flow rate passing through the vessel. *A* is the quadratic flow resistance coefficient representing the effect of elbows and other bends on the pressure drop and *B* is the linear flow resistance coefficient determined by the length and diameter of the vessel. Greater pressure drops will occur with the same amount of mass flow rate through arteries with greater values of *A* and *B*.

It has already been demonstrated that blood flows obey pipe flow theory (Allan, 1976). Thus, the quantitative relationship between blood flow rates and pressure drops can be obtained via the determination of *A* and *B*. In our current study, the mass flow rate of the STA was adjusted to lie in the range of 20–100 ml/min, in order to allow for calculations of various pressure drops via CFD simulation. Based on the results of the pressure drop regression curve, obtained via the least square method, flow resistance coefficients (*A* and *B*) were determined (Zhang et al., 2012b).

2.5. Statistics

Statistical analyses were performed via use of the commercial statistical software package SPSS (version 17.0), with the results presented as mean ± standard deviation (SD). Differences between the values estimated immediately following surgery and at the follow-up stages, were assessed with an independent-samples *t* test. Pearson correlation tests were used to estimate the correlations between flow resistance, WSS and volumetric flows. Throughout analyses, a significance level of 0.05 was assumed.

3. Results

3.1. Observation of bypass morphological change in 6 months follow-up

The average bypass diameter increased from 1.35 ± 0.47 mm immediately following surgery, to 1.60 ± 0.36 mm at follow-up. Despite this, however, no statistical significance was achieved (*P* > 0.05). The quantitative changes of the narrowest diameter in bypass for eleven cases are listed in Table 1. These changes were not uniform. This is exemplified by cases A and J. Changes in morphology of the bypass for case A are shown in Fig. 1A. At 6 months follow-up, the stenosis present in the middle cerebral recipient vessel immediately following surgery resolved. Fig. 1B depicts the morphological change of the bypass for case J, in which the pre-existing curvature of the STA trunk (marked by circle) had

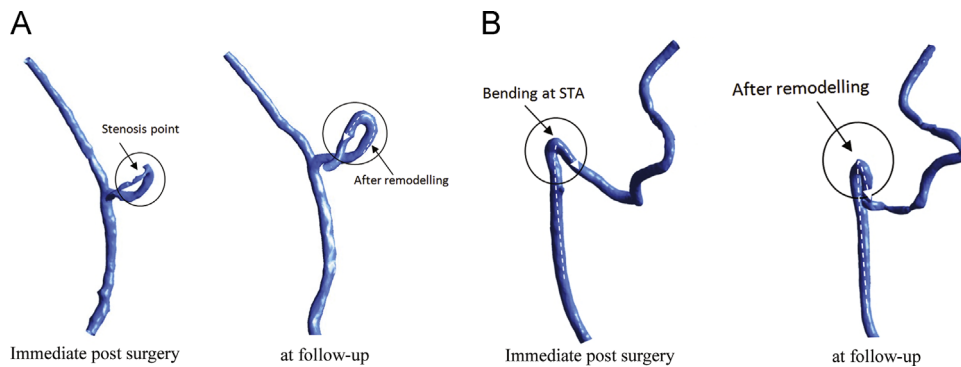


Fig. 1. The morphological alternation of patient A and J. (A) For patient A, vessel stenosis was found at immediate post surgery (left). At follow-up, the pre-existed stenosis was opened up due to the vessel auto-remodelling (right). The configuration of the bypass vessel was remodeled smoothly. (B) For patient J, STA trunk was obviously bended at immediate after surgery (left). At follow-up observation, the bypass was completely shrunk (right). The initial vessel bending may lead the flow change direction and significantly influence the blood perfusion to downstream.

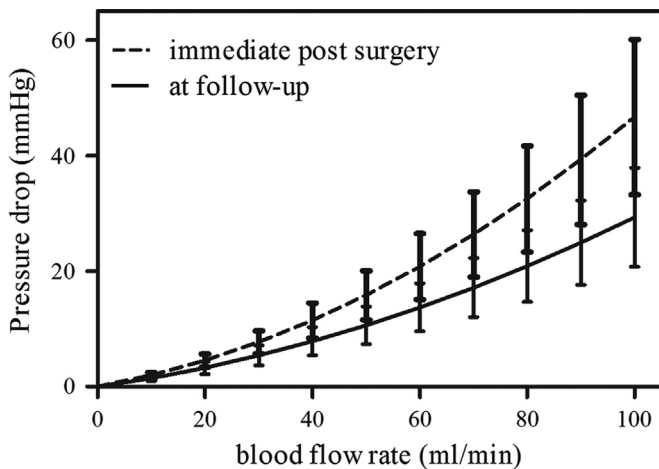


Fig. 2. Flow resistance characteristics at the conditions of immediate post surgery and follow-up.

further increased and the bypass underwent shrinkage at follow-up; reducing its diameter as a result.

3.2. Flow resistance estimation during the 6 months follow-up

The flow resistances of case A–I were reduced at follow-up (Table 1), whilst the average quadratic resistance value of A and linear resistance value of B at the bypass immediately following surgery in nine cases (A–I), was found to be $0.0035 \pm 0.0032 \text{ Pa}/(\text{ml}/\text{min})^2$ and $0.1816 \pm 0.1358 \text{ Pa}/(\text{ml}/\text{min})$, respectively. At 6 months follow-up, A and B were reduced to $0.0015 \pm 0.0016 \text{ Pa}/(\text{ml}/\text{min})^2$ and $0.0844 \pm 0.0483 \text{ Pa}/(\text{ml}/\text{min})$, respectively. The statistical study indicated a significant difference between the values measured immediately following surgery and at 6 months follow-up ($P < 0.05$ for flow resistance values). The reduction in flow resistance at follow-up is shown in Fig. 2. Variations within the patients' group are illustrated by cases A and J. Fig. 3A indicates that the flow resistance at the bypass of case A decreased greatly due to the reduction of stenosis at 6 months follow-up. With a flow condition of 37.7 ml/min, the pressure drop was calculated to be around 10 mmHg. On the other hand, we found an increase in resistances at follow-up analysis, for both case J and case K, an increase attributed to the curvature of the vessel (Fig. 3B, case J). Under the assumed flow condition of 37.7 ml/min, the pressure drop was observed to increase from 9 mmHg to a physiologically improbable 30 mmHg, i.e. the real-flow rate of this bypass must be less than the measured average flow (37.7 ml/min). The results indicated that both vessel curvature and bending will cause high flow resistances in STA

bypass. The STA bypass follow-up flow resistances; A and B, are depicted in Table 1. Flow resistance for cases A–I underwent significant improvement following bypass operation, whilst the volume of A and B appeared to undergo a reduction greater than cases J and K. We must note that though there was reduction of bypass diameters at distal STA for cases D, E, G, and case I at follow up, the flows were measured to increase due to the improvement of flow resistance, especially the reduction of flow elbow and bend resistance coefficient (curvature coefficient) A. The results indicated that the bypass diameter might not be a sole parameter to determine flow resistance.

3.3. Bypass patency examination

We compared the flow rates at the averaged pressure drop from the origin of the STA to the point of bypass anastomosis. Based upon the average mass flow and flow resistances immediately following surgery, we estimated this pressure drop to be at a value of around 10 mmHg. Table 1 reports the flow rates of the bypass immediately following surgery and at follow-up. The mass flow rates of the bypass measured by QMRA increased significantly from $37.72 \pm 14.04 \text{ ml}/\text{min}$ immediately following surgery to $62.55 \pm 28.34 \text{ ml}/\text{min}$ at follow-up ($P < 0.05$). As a result of auto-remodelling (e.g. reduction of stenosis, dilation in diameter, vessel wall smoothing), the flow rate in the bypass increased by about 50% for cases A–I, whilst for cases J and K, the blood flow was reduced by 50% and 25%, respectively. The average resistance coefficients; A and B, as well as shear stress; WSS, were calculated to significantly correlate with STA blood flows. The correlation coefficients found were -0.722 , -0.847 and -0.800 , respectively ($P < 0.01$).

3.4. WSS analysis

Analysis revealed a reduction in WSS at the bypass due to vessel remodelling. The maximum WSS within the bypass was found to be $22.82 \pm 5.02 \text{ Pa}$, falling to $16.91 \pm 5.59 \text{ Pa}$ at follow-up and thereby achieving statistical significance ($P < 0.05$). These reductions in WSS are illustrated in Fig. 4.

Variations within the patient group can be seen throughout cases A and J. As a result of flow-resistance reduction, the maximum WSS occurring at the bypass for case A was likewise reduced. Fig. 5A indicates that the maximum WSS immediately following surgery was approximately 30 Pa, whilst at follow-up, it had reduced to approximately 20 Pa. On the contrary, for case J, the maximum WSS increased from 17 Pa immediately following surgery, to 28 Pa at follow-up (Fig. 5B).

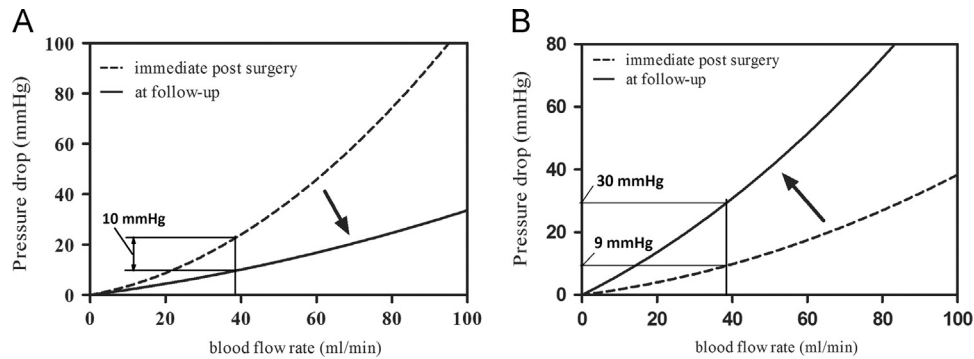


Fig. 3. Flow resistance modulations for patient A and J. (A) For patient A, due to the opening of the pre-existed stenosis, the flow resistance of the STA bypass was reduced by 10 mmHg at the flow rate of 37.7 ml/min at 6 month follow-up. (B) For patient J, due to the shrink of the bypass, the pressure drop was estimated to be increased from 9 mmHg to 30 mmHg at the flow rate of 37.7 ml/min. It is a physiologically improbable condition. In order to maintain the flow perfusion at the bypass at follow-up, the flow must be reduced to much lower than 37.7 ml/min.

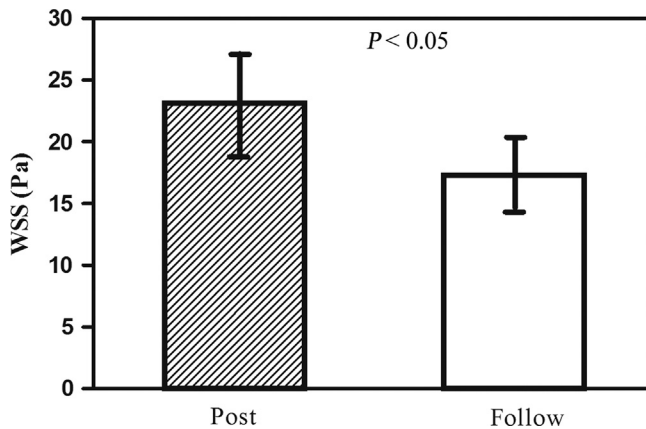


Fig. 4. WSS results. Average WSS was decreased at follow-up. The WSS alternation may also indicate the positive impedance of vessel remodelling.

4. Discussion

4.1. Bypass patency and vessel auto-remodelling

Goldman et al. (2004) reported that the original bypass morphology and graft position significantly modified during the 10 years following coronary bypass surgery. Lajos et al. followed 83 patients who underwent isolated coronary artery bypass surgery with valvular and valveless vein graft and found that venous valves had considerable effect upon the long-term patency of the bypass. As a consequence, they suggested using valveless vein segments whenever possible (Lajos et al., 1996). In cerebrovascular procedure, remodelling of the EC–IC bypass has also been reported. Eguchi (2002) found that the EC–IC bypass diameter alternated within the first 6 months following surgery. Amin-Hanjani et al. (2013) moreover observed a complementary and inverse relationship between the direct bypass graft and indirect revascularization, suggesting that the bypass graft remodels in response to blood demand over time. Even today, the evaluation of intracranial bypass surgery and its patency at follow-up remains empirical. Sia et al. (2011) found that 178 STA–MCA bypasses had excellent long-term patency over many years. Likewise, Gu et al. (2012) demonstrated the occlusion of one of 96 bypasses at the one-year follow-up assessment stage in 53 cases who received combined STA–MCA bypass and EDMS surgery. Though bypass flow is excellent immediately following STA–MCA bypass operations, occlusions may still occur during late follow-up stages. Although this may be related to a number of patient factors, vessel auto-remodelling may play a significant part amongst these causes.

Amid the many physiological mechanisms contributing to this remodelling, the actions of matrix metalloproteinases (MMPs) are considered to have a critical role (Nuki et al., 2009; Ota et al., 2009). Inflammatory cells, such as macrophages, release MMPs in response to blood flow change within vessels. This contributes to the morphological changes of vascular remodelling, characterized by an increase in luminal diameter with relative small changes in wall thickness (Ota et al., 2009). Hemodynamic research has indicated that morphological changes occurring within the bypass are highly dependent upon flow resistance (Zhang et al., 2012a). Our results confirm that vessel auto-remodelling, flow resistance, and blood flow rate are interdependent upon each other.

4.2. STA–MCA bypass flow modulation due to vessel auto-remodelling

In order to further understand the effect of STA–MCA bypass remodelling to adult Moyamoya patients, we have studied STA–MCA bypasses with hemodynamic methodology to measure the flow resistance of coefficients (A and B) at the bypass and test the modifications of bypass patency over a 6-month period. In most cases, the flow resistance of the bypass decreased. Previous studies have shown that the volume of wall shear stress (WSS) is considered to be an important indicator of vessel remodelling (Markl et al., 2010; Shi et al., 1997). Our data illustrates that WSS immediately following surgery tended to be high. This is due to a sudden change in the vascular environment of the STA after incorporation into the bypass. As a consequence of auto-remodelling with time, WSS underwent a reduction. Fig. 5A confirms that for successful cases, WSS tends to be uniform due to the influence of remodelling, a finding that is consistent with previous physiological studies (Gibbons and Dzau, 1994).

In our last 2 cases (case J and case K), WSS and flow resistance increased at follow-up, although patients have yet to exhibit any abnormalities of symptoms during current clinical observations. We speculate that this unexpected remodelling is most likely due to the marked degree of STA curvature at the time of STA–MCA bypass surgery. As discussed above, the initial morphology of the bypass may affect flow distribution inside the vessel, which will further result in differences in vessel remodelling. Our results suggest that bypass with a marked curvature of the STA trunk should be avoided.

To our best knowledge, this is the first study conducted on the haemodynamic analysis of vessel remodelling in STA–MCA bypass for Moyamoya disease using CFD technique. In previous studies, scholars mainly estimated bypass remodeling by observing bypass patency and alterations in angiography at follow-up. There is still a lack of evidence to substantiate the hemodynamic alternations

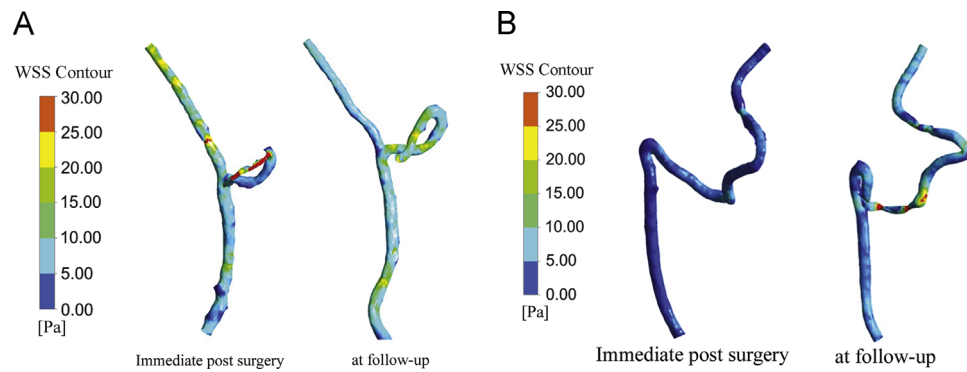


Fig. 5. WSS distribution of patient A and J. (A) For patient A, due to the opening of the stenosis, WSS distribution was improved to be smooth at the follow-up. (B) For patient J, due to the shrink of the bypass, WSS was increased at the follow-up.

seen during bypass remodelling. In this study, we quantitatively investigated vessel auto-remodelling after bypass based on CFD simulations. Our results have confirmed an interdependent relationship between vessel auto-remodelling, flow resistance, and blood flow rate. We also tried to identify the hemodynamic factors which could potentially lead to bypass occlusion, and may thus be useful in clinical application to assist the optimal design of bypass operations in order to maintain the long-term patency of STA-MCA bypass.

4.3. Limitations of the current study

This research analyzed STA-MCA bypass mainly in terms of hemodynamics, rather than clinical outcome. Other factors may also affect long-term bypass patency in spite of vessel auto-remodelling; e.g. the actual demand of blood flow, collateral development from indirect revascularization, blood coagulation status and medication protocol. We were not able to distinguish the impacts of these factors in this study. Another limitation of this study is that the number of cases is small. To fully elucidate the nature of auto-remodelling, further investigation is required.

5. Conclusion

This research investigates STA-MCA bypass auto-remodelling for adult Moyamoya patients. For most STA-MCA bypasses, vessel auto-remodelling reduced stenoses present within the recipient artery immediately after surgery and increased the uniformity of internal diameter with time. As a result, the flow resistance of the bypass is reduced, with increased flow rate and increasingly uniform WSS. Our results also highlight the significance of the initial bypass morphology in the auto-remodelling process. If the STA trunk possesses marked curvature, the auto-remodelling may be associated with a worsening of the pre-existing curvature, increasing flow resistance and, potentially, vessel occlusion. To ensure optimal STA-MCA bypass at follow-up, both the curvature and lie of the bypass vessel must be carefully considered.

Conflict of interest statement

None of the authors have any financial interests to disclose.

Acknowledgement

This study was sponsored by Australian Research Council Discovery Project DP1112985, Ministry of Health of the People's

Republic of China 2011BAI08B06, and SHDC12010118 from Shanghai Hospital Developing Center, China.

References

- Allan, C.R., 1976. Effect of collateral and peripheral resistance on blood flow through arterial stenoses. *J. Biomech.* 9, 367–375.
- Amin-Hanjani, S., Shin, J.H., Zhao, M., Du, X., Charbel, F.T., 2007. Evaluation of extracranial–intracranial bypass using quantitative magnetic resonance angiography. *J. Neurosurg.* 106, 291–298.
- Amin-Hanjani, S., Singh, A., Rifai, H., Thulborn, K.R., Alaraj, A., Aletich, V., Charbel, F. T., 2013. Combined direct and indirect bypass for Moyamoya: quantitative assessment of direct bypass flow over time. *Neurosurgery*.
- Brater, F.E., King, H.W. (Eds.), 1976. *Handbook of Hydraulics for the Solution of Hydraulic Engineering Problems*. McGraw-Hill, New York.
- Eguchi, T., 2002. EC/IC bypass using a long-vein graft. *Int. Congr. Ser.* 1247, 421–435.
- Fukui, M., 1997. Current state of study on Moyamoya disease in Japan. *Surg. Neurol.* 47, 138–143.
- Gibbons, G.H., Dzau, V.J., 1994. The emerging concept of vascular remodeling. *N. Engl. J. Med.* 330, 1431–1438.
- Goldman, S., Zadina, K., Moritz, T., Ovit, T., Sethi, G., Copeland, J.G., Thottapurathu, L., Krasnicka, B., Ellis, N., Anderson, R.J., Henderson, W., 2004. Long-term patency of saphenous vein and left internal mammary artery grafts after coronary artery bypass surgery: results from a Department of Veterans Affairs Cooperative Study. *J. Am. Coll. Cardiol.* 44, 2149–2156.
- Gu, Y., Ni, W., Jiang, H., Ning, G., Xu, B., Tian, Y., Xu, F., Liao, Y., Song, D., Mao, Y., 2012. Efficacy of extracranial–intracranial revascularization for non-moyamoya steno-occlusive cerebrovascular disease in a series of 66 patients. *J. Clin. Neurosci.* 19, 1408–1415.
- Jamali, A.A., Deuel, C., Perreira, A., Salgado, C.J., Hunter, J.C., Strong, E.B., 2007. Linear and angular measurements of computer-generated models: are they accurate, valid, and reliable? *Comput.-Aided Surg.: Off. J. Int. Soc. Comput.-Aided Surg.* 12, 278–285.
- Kim, M., Taulbee, D.B., Tremmel, M., Meng, H., 2008. Comparison of two stents in modifying cerebral aneurysm hemodynamics. *Ann. Biomed. Eng.* 36, 726–741.
- Kuroda, S., Houkin, K., 2008. Moyamoya disease: current concepts and future perspectives. *Lancet Neurol.* 7, 1056–1066.
- Lajos, T.Z., Graham, S.P., Guntupalli, M., Raza, S.T., Hasnain, S., 1996. Comparison of long-term patency of “horseshoe” saphenous vein grafts with and without valves. *Eur. J. Cardiothorac. Surg.: Off. J. Eur. Assoc. Cardiothorac. Surg.* 10, 846–851.
- Markl, M., Wegent, F., Zech, T., Bauer, S., Strecker, C., Schumacher, M., Weiller, C., Hennig, J., Harloff, A., 2010. In vivo wall shear stress distribution in the carotid artery: effect of bifurcation geometry, internal carotid artery stenosis, and recanalization therapy. *Circulation Cardiovasc. Imaging* 3, 647–655.
- Nuki, Y., M.M., Tsang, E., Young, W.L., van Rooijen, N., Kurihara, C., Hashimoto, T., 2009. Roles of macrophages in flow-induced outward vascular remodeling. *J. Cereb. Blood Flow Metab.* 29, 495–503.
- Ota, R., Kurihara, C., Tsou, T.L., Young, W.L., Yeghiazarians, Y., Chang, M., Mobashery, S., Sakamoto, A., Hashimoto, T., 2009. Roles of matrix metalloproteinases in flow-induced outward vascular remodeling. *J. Cereb. Blood Flow Metab.: Off. J. Int. Soc. Cereb. Blood Flow Metab.* 29, 1547–1558.
- Qian, Y., Itatani, L.J., Miyaji, K., Umezumi, M., K., 2010. Computational hemodynamic analysis in congenital heart disease: simulation of the Norwood procedure. *Ann. Biomed. Eng.* 38, 2302–2313.
- Shi, Z.D., Winoto, S.H., Lee, T.S., 1997. Experimental investigation of pulsatile flows in tubes. *J. Biomech. Eng.* 119, 213–216.
- Sia, S.F., Davidson, A.S., Assaad, N.N., Stoodley, M., Morgan, M.K., 2011. Comparative patency between intracranial arterial pedicle and vein bypass surgery. *Neurosurgery* 69, 308–314.
- Suzuki, J., Takaku, A., 1969. Cerebrovascular ‘Moyamoya disease’: a disease showing abnormal net-like vessels in base of brain. *Arch. Neurol.* 20, 288–299.

- Takeuchi, K., Shimizu, K., 1957. Hypoplasia of the bilateral internal carotid arteries. *No To Shinkei* 9, 37–43.
- Xu, B., Song, D.L., Mao, Y., Gu, Y.X., Xu, H., Liao, Y.J., Liu, C.H., Zhou, L.F., 2012. Superficial temporal artery-middle cerebral artery bypass combined with encephalo-duro-myo-synangiosis in treating Moyamoya disease: surgical techniques, indications and midterm follow-up results. *Chin. Med. J. (Engl.)* 125, 4398–4405.
- Zhang, Y., Furusawa, T., Sia, S.F., Umezu, M., Qian, Y., 2012a. Proposition of an outflow boundary approach for carotid artery stenosis CFD simulation. *Comput. Meth. Biomech. Biomed. Eng.*
- Zhang, Y., Sia, S.F., Morgan, M.K., Qian, Y., 2012b. Flow resistance analysis of extracranial-to-intracranial (EC-IC) vein bypass. *J. Biomech.*
- Zhao, M., Amin-Hanjani, S., Ruland, S., Curcio, A.P., Ostergren, L., Charbel, F.T., 2007. Regional cerebral blood flow using quantitative MR angiography. *AJNR Am. J. Neuroradiol.* 28, 1470–1473.